

Nucleon structure in a light-front quark model consistent with quark counting rules and data

Thomas Gutsche,¹ Valery E. Lyubovitskij,^{1,2,3} Ivan Schmidt,⁴ and Alfredo Vega^{5,6}

¹*Institut für Theoretische Physik, Universität Tübingen, Kepler Center for Astro and Particle Physics, Auf der Morgenstelle 14, D-72076 Tübingen, Germany*

²*Department of Physics, Tomsk State University, 634050 Tomsk, Russia*

³*Mathematical Physics Department, Tomsk Polytechnic University, Lenin Avenue 30, 634050 Tomsk, Russia*

⁴*Departamento de Física y Centro Científico Tecnológico de Valparaíso (CCTVal), Universidad Técnica Federico Santa María, Casilla 110-V, Valparaíso, Chile*

⁵*Instituto de Física y Astronomía, Universidad de Valparaíso, Avenida Gran Bretaña 1111, Valparaíso, Chile*

⁶*Centro de Astrofísica de Valparaíso, Avenida Gran Bretaña 1111, Valparaíso, Chile*
(Received 10 November 2014; published 23 March 2015)

Using global fits of valence u and d quark parton distributions and data on quark and nucleon form factors in the Euclidean region, we derive a light-front quark model for the nucleon structure consistent with quark counting rules.

DOI: [10.1103/PhysRevD.91.054028](https://doi.org/10.1103/PhysRevD.91.054028)

PACS numbers: 12.38.Lg, 13.40.Gp, 14.20.Dh, 14.65.Bt

I. INTRODUCTION

The main objective of this paper is to continue our study of a phenomenological light-front wave function (LFWF) for the nucleon started as in Ref. [1]. We derived a LFWF for hadrons for both pions and nucleons which at an initial scale is constrained by the soft-wall anti-de Sitter (AdS)/QCD model, and which at higher scales gives the correct scaling behavior of parton distributions and form factors. The explicit form of the wave function at large scales is extracted from the hard evolution of parton distribution functions (PDFs) and generalized parton distributions (GPDs). The proposed wave function produces form factors consistent with quark counting rules [2] and also gives predictions for the corresponding parton distributions. In our considerations we obtained harder PDFs in comparison with the results of global fits [see e.g. results of Martin, Stirling, Thorne and Watt (MSTW) [3]]. The reason for a softening of the PDFs was discussed in the pion case in Ref. [4]. There it was clearly demonstrated that the inclusion of next-to-leading logarithmic threshold resummation effects, due to collinear and soft gluon contributions, leads to a softer pion PDF [4]. This result also shows that we should take into account these resummation effects and derive an improved nucleon LFWF. In Ref. [5] we demonstrate how to derive in the case of the pion a LFWF producing a softer PDF as in Ref. [4] and a pionic electromagnetic form factor consistent with data and quark counting rules. Here we extend this idea to the case of the nucleon. We propose a LFWF for the nucleon modeled as a quark-scalar diquark bound state, with a specific dependence on the transverse momentum \mathbf{k}_\perp and the light-cone variable x . This LFWF produces PDFs for the valence u and d quarks

found in the global fits of Ref. [3]. It also describes the electromagnetic form factors of the nucleon including their flavor decomposition into u and d quark form factors up to values of the momentum transfer squared $Q^2 = 30 \text{ GeV}^2$ in the Euclidean region (for a recent overview of experimental and theoretical progress in the study of nucleon electromagnetic structure see e.g. Refs. [6–8]). It is important to stress that the calculated nucleon electromagnetic form factors are consistent with quark counting rules for large values of Q^2 .

The main advantage of our approach is that the derived LFWF does not depend on phenomenological parameters like masses of quark/diquark, which are not directly related to QCD. Restricting to zero current quark masses we obtain a reasonable description of data on nucleon form factors. Note, we derive the LFWF at the initial scale $\mu_0 = 1 \text{ GeV}$ producing corresponding PDFs at the same scale. Both quantities are scale dependent. We showed explicitly in our paper [1] that at any scale evolved PDF could constraint the corresponding LFWF. The most convenient way is to set up the LFWF at the initial scale, calculate the corresponding PDF and then perform an evolution of the PDF to higher scales. On the other hand, as we stressed before, we make a further improvement on the light-front quark model for a nucleon proposed in Ref. [1] producing softer quark PDFs at the initial scale $\mu_0 = 1 \text{ GeV}$ in agreement with a global analysis of these quantities from the data (see details in Sec. II). The description of nucleon structure starting from light-front wave functions is also our improvement in comparison with other approaches calculating nucleon form factors using parametrization for generalized parton distributions [9].

II. LIGHT-FRONT QUARK-DIQUARK MODEL FOR THE NUCLEON

In this section we propose a phenomenological LFWF $\psi(x, \mathbf{k}_\perp)$ for the nucleon, set up as a bound state of an active quark and a spectator scalar diquark. This LFWF is able to produce the u and d quark PDFs derived in the global fits of Ref. [3] and generates electromagnetic form factors of nucleons including their flavor decomposition which are consistent with data.

First we collect the well-known decompositions [10] of the nucleon Dirac and Pauli form factors $F_{1,2}^N$ ($N = p, n$) in terms of the valence quark distributions in nucleons with $F_{1,2}^q$ ($q = u, d$), which then are related to the GPDs (\mathcal{H}^q and \mathcal{E}^q) [11] of valence quarks

$$\begin{aligned} F_i^{p(n)}(Q^2) &= \frac{2}{3} F_i^{u(d)}(Q^2) - \frac{1}{3} F_i^{d(u)}(Q^2), \\ F_1^q(Q^2) &= \int_0^1 dx \mathcal{H}^q(x, Q^2), \\ F_2^q(Q^2) &= \int_0^1 dx \mathcal{E}^q(x, Q^2). \end{aligned} \quad (1)$$

At $Q^2 = 0$ the GPDs are related to the quark densities—valence $q_v(x)$ and magnetic $\mathcal{E}_q(x)$ as

$$\mathcal{H}^q(x, 0) = q_v(x), \quad \mathcal{E}^q(x, 0) = \mathcal{E}^q(x), \quad (2)$$

which are normalized as

$$\begin{aligned} n_q &= F_1^q(0) = \int_0^1 dx q_v(x), \\ \kappa_q &= F_2^q(0) = \int_0^1 dx \mathcal{E}^q(x). \end{aligned} \quad (3)$$

The number of u or d valence quarks in the proton is denoted by n_q , and κ_q is the quark anomalous magnetic moment.

Next we recall the definitions of the nucleon Sachs form factors $G_{E/M}^N(Q^2)$ and the electromagnetic radii $\langle r_{E/M}^2 \rangle^N$ in terms of the Dirac and Pauli form factors

$$\begin{aligned} G_E^N(Q^2) &= F_1^N(Q^2) - \frac{Q^2}{4m_N^2} F_2^N(Q^2), \\ G_M^N(Q^2) &= F_1^N(Q^2) + F_2^N(Q^2), \\ \langle r_E^2 \rangle^N &= -6 \frac{dG_E^N(Q^2)}{dQ^2} \Big|_{Q^2=0}, \\ \langle r_M^2 \rangle^N &= -\frac{6}{G_M^N(0)} \frac{dG_M^N(Q^2)}{dQ^2} \Big|_{Q^2=0}, \end{aligned} \quad (4)$$

where $G_M^N(0) \equiv \mu_N$ is the nucleon magnetic moment.

The light-front representation [12,13] for the Dirac and Pauli quark form factors is

$$\begin{aligned} F_1^q(Q^2) &= \int_0^1 dx \int \frac{d^2 \mathbf{k}_\perp}{16\pi^3} [\psi_{+q}^{+*}(x, \mathbf{k}'_\perp) \psi_{+q}^+(x, \mathbf{k}_\perp) \\ &\quad + \psi_{-q}^{+*}(x, \mathbf{k}'_\perp) \psi_{-q}^+(x, \mathbf{k}_\perp)], \end{aligned} \quad (5)$$

$$\begin{aligned} F_2^q(Q^2) &= -\frac{2M_N}{q^1 - iq^2} \int_0^1 dx \int \frac{d^2 \mathbf{k}_\perp}{16\pi^3} \\ &\quad \times [\psi_{+q}^{+*}(x, \mathbf{k}'_\perp) \psi_{+q}^-(x, \mathbf{k}_\perp) \\ &\quad + \psi_{-q}^{+*}(x, \mathbf{k}'_\perp) \psi_{-q}^-(x, \mathbf{k}_\perp)]. \end{aligned} \quad (6)$$

Here M_N is the nucleon mass, $\psi_{\lambda_q}^{\lambda_N}(x, \mathbf{k}_\perp)$ are the LFWFs at the initial scale μ_0 with specific helicities for the nucleon $\lambda_N = \pm$ and for the struck quark $\lambda_q = \pm$, where plus and minus correspond to $+\frac{1}{2}$ and $-\frac{1}{2}$, respectively. We work in the frame with $q = (0, 0, \mathbf{q}_\perp)$, and where the Euclidean momentum squared is $Q^2 = \mathbf{q}_\perp^2$. As the initial scale we choose the value $\mu_0 = 1$ GeV which is used in the MSTW global fit [3].

In the quark-scalar diquark model, the generic ansatz for the massless LFWFs at the initial scale $\mu_0 = 1$ GeV reads

$$\begin{aligned} \psi_{+q}^+(x, \mathbf{k}_\perp) &= \varphi_q^{(1)}(x, \mathbf{k}_\perp), \\ \psi_{-q}^+(x, \mathbf{k}_\perp) &= -\frac{k^1 + ik^2}{xM_N} \varphi_q^{(2)}(x, \mathbf{k}_\perp), \\ \psi_{+q}^-(x, \mathbf{k}_\perp) &= \frac{k^1 - ik^2}{xM_N} \varphi_q^{(2)}(x, \mathbf{k}_\perp), \\ \psi_{-q}^-(x, \mathbf{k}_\perp) &= \varphi_q^{(1)}(x, \mathbf{k}_\perp), \end{aligned} \quad (7)$$

where $\varphi_q^{(1)}$ and $\varphi_q^{(2)}$ are the twist-3 LFWFs. They are generalizations of the twist-3 LFWFs found from matching the electromagnetic form factors of the nucleon in soft-wall AdS/QCD [14–18] and light-front QCD (see the detailed discussion in Ref. [1]). In particular, as a result of the matching the following LFWFs have been deduced:

$$\begin{aligned} \varphi_q^{\text{AdS/QCD}(i)}(x, \mathbf{k}_\perp) &= N_q^{(i)} \frac{4\pi}{\kappa} \sqrt{\frac{\log(1/x)}{1-x}} \exp\left[-\frac{\mathbf{k}_\perp^2 \log(1/x)}{2\kappa^2 (1-x)^2}\right], \end{aligned} \quad (8)$$

where the $N_q^{(i)}$ are normalization constants fixed by the conditions of (3). Note that the derived LFWF is not symmetric under the exchange $x \rightarrow 1-x$. This is the case because it was extracted from a matching of matrix elements of the bare electromagnetic current between the dressed LFWF in light-front QCD and of the dressed electromagnetic current between hadronic wave functions in AdS/QCD.

The generalization $\varphi_q^{\text{AdS/QCD}(i)}(x, \mathbf{k}_\perp) \rightarrow \varphi_q^{(i)}(x, \mathbf{k}_\perp)$ is encoded in the longitudinal factors $f_q^{(i)}(x)$ and $\bar{f}_q(x)$ which take into account collinear and soft gluon effects as

$$\begin{aligned} \varphi_q^{(i)}(x, \mathbf{k}_\perp) &= N_q^{(i)} \frac{4\pi}{\kappa} \sqrt{\frac{\log(1/x)}{1-x}} \sqrt{f_q^{(i)}(x) \bar{f}_q(x)} \\ &\times \exp \left[-\frac{\mathbf{k}_\perp^2}{2\kappa^2} \frac{\log(1/x)}{(1-x)^2} \bar{f}_q(x) \right]. \end{aligned} \quad (9)$$

These factors lead to softer PDFs, which coincide with the results of the global fit performed e.g. in Ref. [3]. At the same time, the power scaling of electromagnetic form factors for large values of Euclidean momentum squared with $Q^2 \rightarrow \infty$ remains the same up to power-scaling breaking corrections $\Delta_q^{(i)}$ [see Eqs. (18) and (20)], which produce fine-tuned fits of the nucleon electromagnetic form factors, i.e. consistent with quark counting rules. The choice of the functions $f_q^{(i)}(x)$ is constrained by the valence u and d quark PDF, while $\bar{f}_q(x)$ is fixed from the fit to quark and nucleon form factors. The functions $f_q^{(i)}(x)$ and $\bar{f}_q(x)$ are specified as

$$\begin{aligned} f_q^{(1)}(x) &= x^{\eta_q^{(1)}-1} (1-x)^{\eta_q^{(2)}-1} (1 + \epsilon_q \sqrt{x} + \gamma_q x), \\ f_q^{(2)}(x) &= x^{2+\rho_q} (1-x)^{\sigma_q} (1 + \lambda_q \sqrt{x} + \delta_q x)^2 f_q^{(1)}(x), \\ \bar{f}_q(x) &= x^{\bar{\eta}_q^{(1)}} (1-x)^{\bar{\eta}_q^{(2)}} (1 + \bar{\epsilon}_q \sqrt{x} + \bar{\gamma}_q x), \end{aligned} \quad (10)$$

where the parameters $\eta_q^{(1)}$, $\eta_q^{(2)}$, ϵ_q and γ_q are fixed from the global MSTW analysis of Ref. [3] (for simplicity we restrict ourselves to leading-order results). The parameters ρ_q , σ_q , λ_q , δ_q , $\bar{\eta}_q^{(1)}$, $\bar{\eta}_q^{(2)}$, $\bar{\epsilon}_q$ and $\bar{\gamma}_q$ are fixed from a fit to the anomalous magnetic moments of quarks (nucleons) and to the Q^2 dependence of the electromagnetic quark (nucleon) form factors. The final set of parameters specifying the functions $f_q^{(i)}(x)$ and $\bar{f}_q(x)$ is listed in Table I.

The scale parameter $\kappa = 350$ MeV remains the same as fixed in the analysis of Ref. [1] and used in the analysis for the pion of Ref. [5]. The parameter κ is related to the

TABLE I. Parameters specifying $f_q^{(i)}(x)$ and $\bar{f}_q(x)$.

Parameter	Value	Parameter	Value
$\eta_u^{(1)}$	0.45232	$\eta_d^{(1)}$	0.71978
$\eta_u^{(2)}$	3.0409	$\eta_d^{(2)}$	5.3444
ϵ_u	-2.3737	ϵ_d	-4.3654
γ_u	8.9924	γ_d	7.4730
$\bar{\eta}_u^{(1)}$	0.195	$\bar{\eta}_d^{(1)}$	0.280
$\bar{\eta}_u^{(2)}$	$\frac{\eta_u^{(2)}-1}{2} - 0.54$	$\bar{\eta}_d^{(2)}$	$\frac{\eta_d^{(2)}-1}{2} - 0.60$
$\bar{\epsilon}_u$	-0.71	$\bar{\epsilon}_d$	-0.10
$\bar{\gamma}_u$	0	$\bar{\gamma}_d$	0
ρ_u	0.091	ρ_d	-0.17
σ_u	$(\eta_u^{(2)} - 1) - 0.2409$	σ_d	$(\eta_d^{(2)} - 1) - 2.3444$
λ_u	-2.40	λ_d	-0.22
δ_u	3.18	δ_d	3.90

scale parameter of the background dilaton field providing confinement and is universal for all hadronic wave functions.

The expressions for the quark PDFs read

$$\begin{aligned} q_v(x) &= (N_q^{(1)})^2 (1-x) f_q^{(1)}(x) \\ &+ (N_q^{(2)})^2 \frac{\kappa^2}{M_N^2 x^2} \frac{(1-x)^3}{\log(1/x)} \frac{f_q^{(2)}(x)}{\bar{f}_q(x)}, \end{aligned} \quad (11)$$

$$\mathcal{E}^q(x) = 2N_q^{(1)} N_q^{(2)} \frac{(1-x)^2}{x} \sqrt{f_q^{(1)}(x) f_q^{(2)}(x)}. \quad (12)$$

The ratio $c_q = N_q^{(2)}/N_q^{(1)}$ is a free parameter and we choose for simplicity $c_u = 1$ and $c_d = -1$ or $N_u^{(1)} = N_u^{(2)} = N_u$ and $N_d^{(1)} = -N_d^{(2)} = N_d$. In our calculations normalization constants N_u and N_d are fixed as $N_u = 1.18093$ and $N_d = 2.00432$. Notice that the contribution of the struck quark with negative helicity $\lambda_q = -$ [see the second term in Eq. (11)] to the quark PDFs $q_v(x)$ is relatively suppressed by a factor $\kappa^2/M_N^2 \sim 1/10$. To match the $u_v(x)$ and $d_v(x)$ PDFs fixed in the global fit of Ref. [3], we slightly change the parameters in the longitudinal factor $f_q(x)$. We found that in the case of the PDF $u_v(x)$ the contribution of the struck quark with negative helicity is negligible. In the case of the PDF $d_v(x)$ we slightly change the parameter $\eta_d^{(2)} = 5.1244$ fixed in Ref. [3] to $\eta_d^{(2)} = 5.3444$ to match the results of the global fit in [3].

Expressions for the quark helicity-independent GPDs \mathcal{H}^q and \mathcal{E}^q in the nucleon read

$$\begin{aligned} \mathcal{H}^q(x, Q^2) &= q_v(x, Q^2) \exp \left[-\frac{Q^2}{4\kappa^2} \log(1/x) \bar{f}_q(x) \right], \\ q_v(x, Q^2) &= q_v(x) - (N_q^{(2)})^2 \frac{Q^2}{4M_N^2} \frac{(1-x)^3}{x^2} f_q^{(2)}(x), \\ \mathcal{E}^q(x, Q^2) &= \mathcal{E}^q(x) \exp \left[-\frac{Q^2}{4\kappa^2} \log(1/x) \bar{f}_q(x) \right]. \end{aligned} \quad (13)$$

In the following we consider the scaling of the PDFs at large x and form factors at large Q^2 . The $q_v(x)$ scale at large x as

$$\begin{aligned} q_v(x) &\sim (1-x)^{\eta_q^{(2)}}, \\ u_v(x) &\sim (1-x)^3, \\ d_v(x) &\sim (1-x)^5. \end{aligned} \quad (14)$$

For the $\mathcal{E}^q(x)$ we have the scaling behavior at large x as

$$\begin{aligned} \mathcal{E}^q(x) &\sim q_v(x) (1-x)^{1+\sigma_q/2} \sim (1-x)^{\eta_q^{(2)}+1+\sigma_q/2}, \\ \mathcal{E}^u(x) &\sim (1-x)^5, \quad \mathcal{E}^d(x) \sim (1-x)^7. \end{aligned} \quad (15)$$

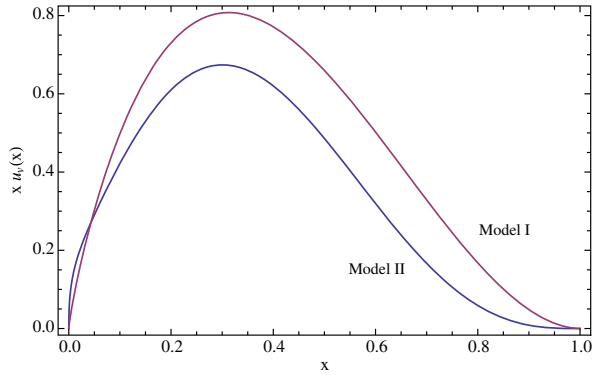


FIG. 1 (color online). $u_v(x)$ at scale $\mu = 1$ GeV in models I and II.

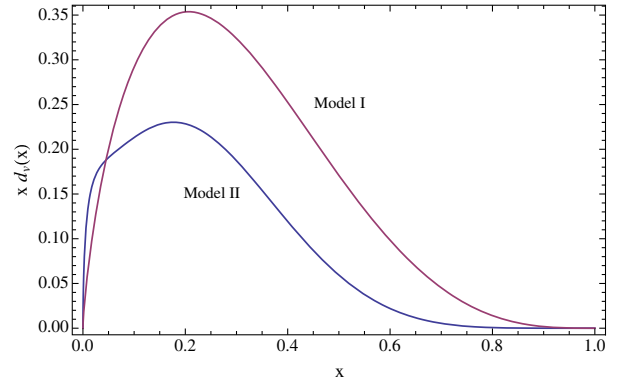


FIG. 4 (color online). $d_v(x)$ at scale $\mu = 10$ GeV in models I and II.

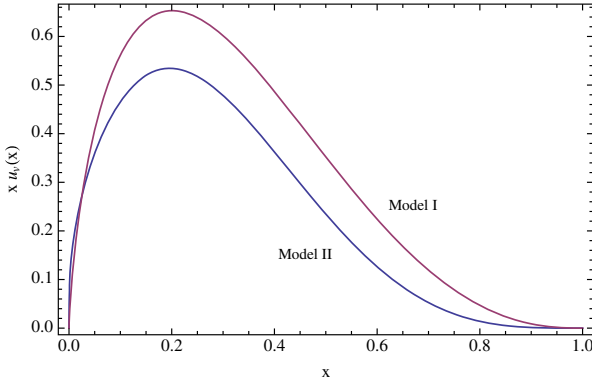


FIG. 2 (color online). $u_v(x)$ at scale $\mu = 10$ GeV in models I and II.

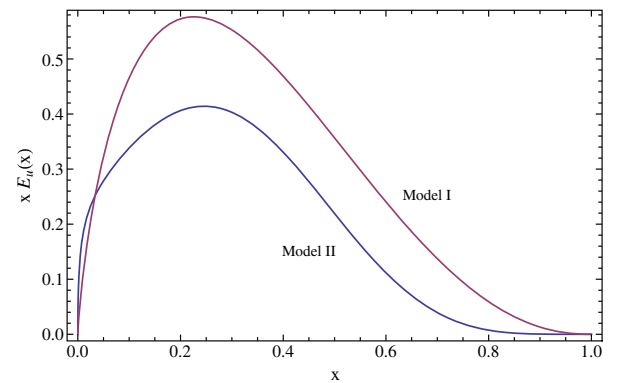


FIG. 5 (color online). $\mathcal{E}_u(x)$ at scale $\mu = 1$ GeV in models I and II.

Note that in the case of the u quark PDFs our results are consistent with perturbative QCD [19,20]. The d quark PDFs have an additional power of 2 in the scaling behavior as required by the global analysis. As we mentioned before the scaling of the quark PDFs calculated in this paper is softer at the initial scale $\mu_0 = 1$ GeV in comparison with results of Ref. [1], where we considered another version of the present light-front quark model. In particular,

the PDFs calculated in Ref. [1] scale $u_v(x) \sim (1-x)^2$, $d_v(x) \sim (1-x)^{2.5}$, $\mathcal{E}^u(x) \sim (1-x)^{2.3}$ and $\mathcal{E}^d(x) \sim (1-x)^{2.8}$. Note that the quality of the description of nucleon electromagnetic form factors is similar in both versions of our approach. Therefore, the main advantage of the present version of our approach in comparison with the version discussed in Ref. [1] consists in the improvement of the behavior of quark PDFs. In Figs. 1–8 we perform a

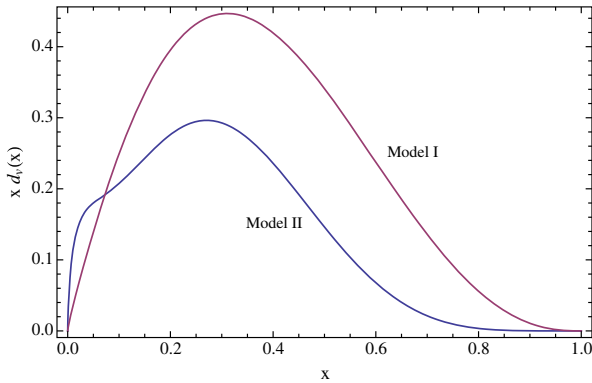


FIG. 3 (color online). $d_v(x)$ at scale $\mu = 1$ GeV in models I and II.

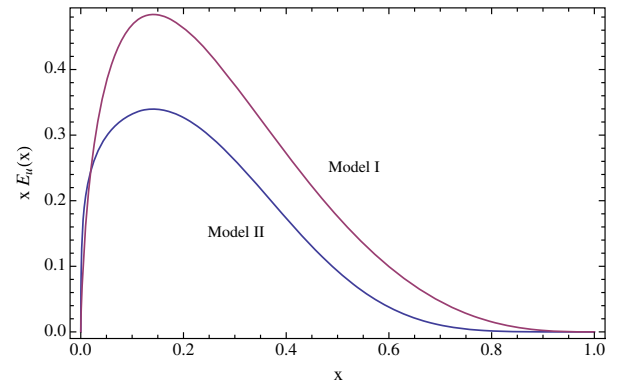
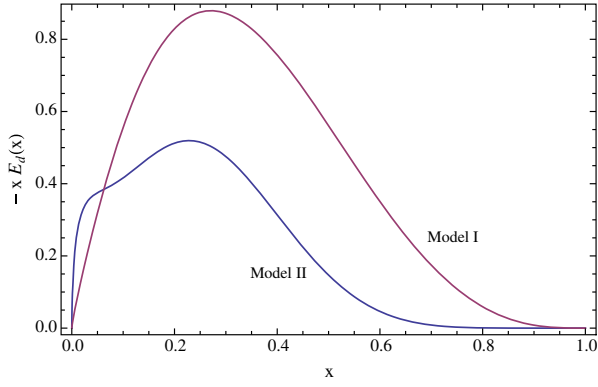
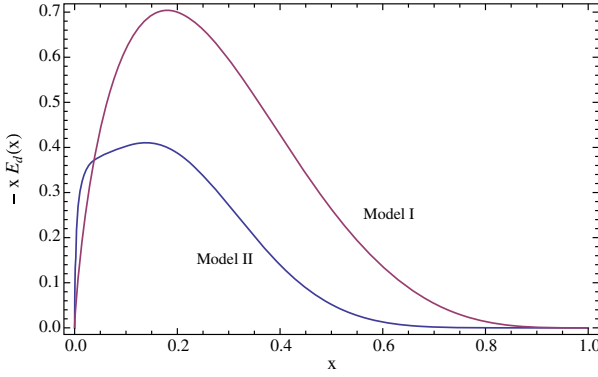


FIG. 6 (color online). $\mathcal{E}_u(x)$ at scale $\mu = 10$ GeV in models I and II.


 FIG. 7 (color online). $\mathcal{E}_d(x)$ at scale $\mu = 1$ GeV in models I and II.

 FIG. 8 (color online). $\mathcal{E}_d(x)$ at scale $\mu = 10$ GeV in models I and II.

comparison of PDFs calculated in two versions of our approach (model I discussed in Ref. [1] and model II proposed in the present paper). For convenience, we present results for the quark PDFs at scales 1 and 10 GeV.

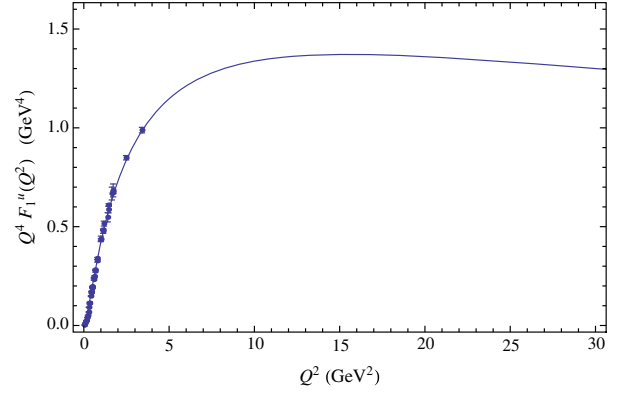
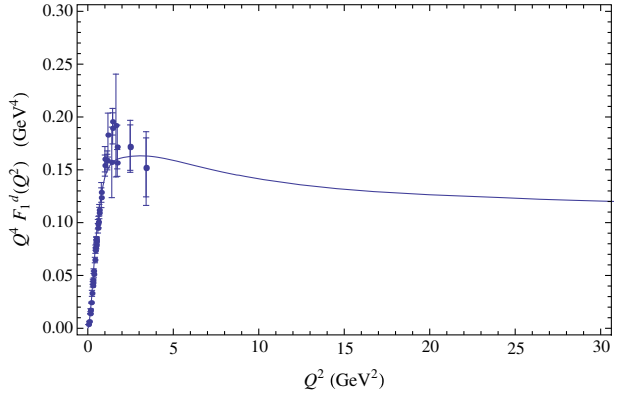
In the case of the nucleon form factors we get for large Q^2 the behaviors

$$\begin{aligned}
 F_1^q(Q^2) &\sim \int_0^1 dx (1-x)^{\eta_q^{(2)}} \exp\left[-\frac{Q^2}{4\kappa^2} (1-x)^{1+\bar{\eta}_q^{(2)}}\right] \\
 &\sim \left(\frac{1}{Q^2}\right)^{\frac{1+\eta_q^{(2)}}{1+\bar{\eta}_q^{(2)}}} \sim \left(\frac{1}{Q^4}\right)^{1+\Delta_q^{(1)}} \quad (16)
 \end{aligned}$$

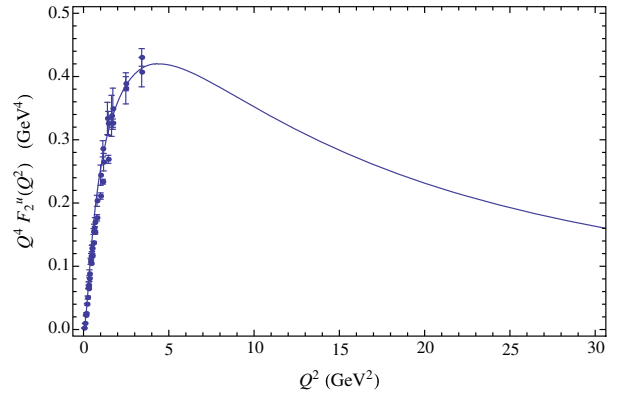
and

TABLE II. Electromagnetic properties of nucleons.

Quantity	Our results	Data [22]
μ_p (in n.m.)	2.793	2.793
μ_n (in n.m.)	-1.913	-1.913
r_E^p (fm)	0.781	$0.84087 \pm 0.00026 \pm 0.00029$
$\langle r_E^2 \rangle^n$ (fm ²)	-0.112	-0.1161 ± 0.0022
r_M^p (fm)	0.717	$0.777 \pm 0.013 \pm 0.010$
r_M^n (fm)	0.694	$0.862^{+0.009}_{-0.008}$


 FIG. 9 (color online). Dirac u quark form factor multiplied by Q^4 .

 FIG. 10 (color online). Dirac d quark form factor multiplied by Q^4 .

$$\begin{aligned}
 F_2^q(Q^2) &\sim \int_0^1 dx (1-x)^{1+\eta_q^{(2)}+\sigma_q/2} \\
 &\quad \times \exp\left[-\frac{Q^2}{4\kappa^2} (1-x)^{1+\bar{\eta}_q^{(2)}}\right] \\
 &\sim \left(\frac{1}{Q^2}\right)^{\frac{2+\eta_q^{(2)}+\sigma_q/2}{1+\bar{\eta}_q^{(2)}}} \sim \left(\frac{1}{Q^6}\right)^{1+\Delta_q^{(2)}}. \quad (17)
 \end{aligned}$$


 FIG. 11 (color online). Pauli u quark form factor multiplied by Q^4 .

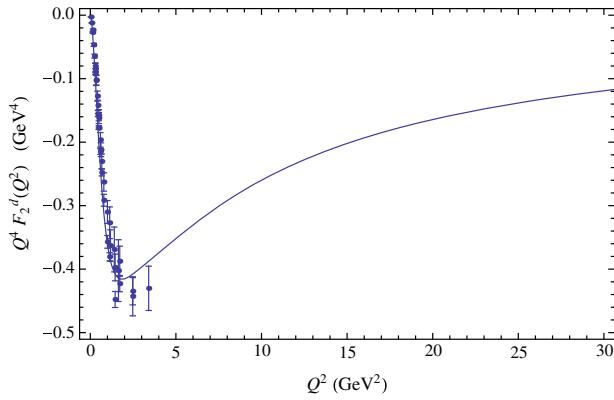


FIG. 12 (color online). Pauli d quark form factor multiplied by Q^4 .

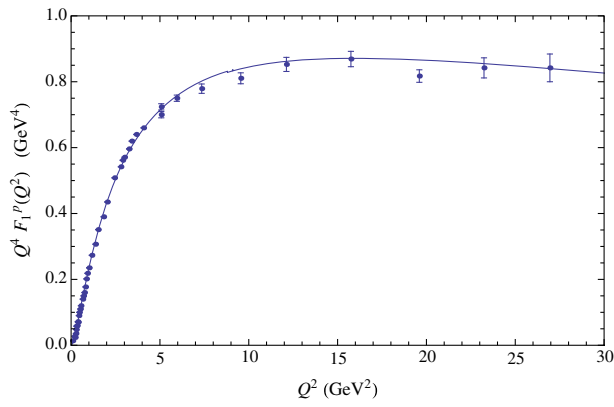


FIG. 13 (color online). Dirac proton form factor multiplied by Q^4 .

Here, the $\Delta_q^{(1)}$ and $\Delta_q^{(2)}$ are the small corrections encoding a deviation of the Dirac and Pauli quark form factors from the power-scaling laws $1/Q^4$ and $1/Q^6$, respectively. These corrections are given in the form

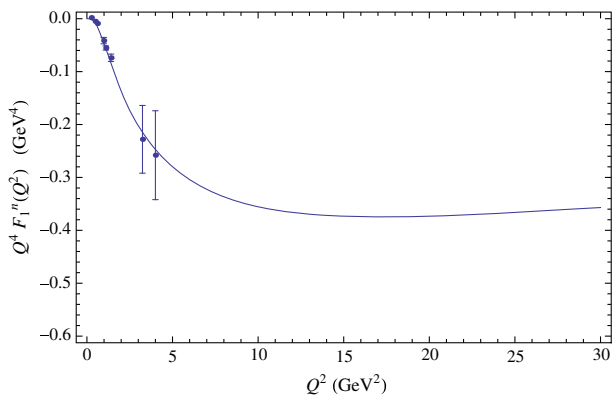


FIG. 14 (color online). Dirac neutron form factor multiplied by Q^4 .

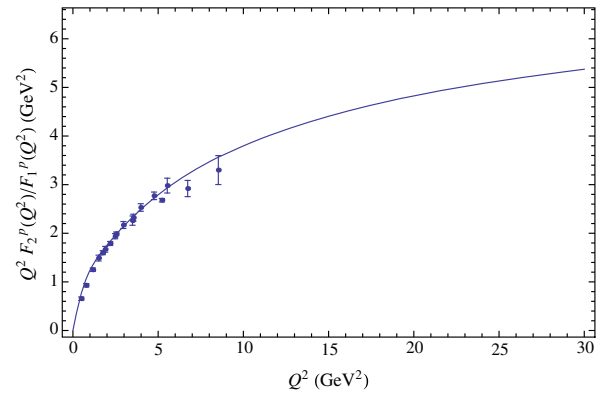


FIG. 15 (color online). Ratio $Q^2 F_2^p(Q^2)/F_1^p(Q^2)$.

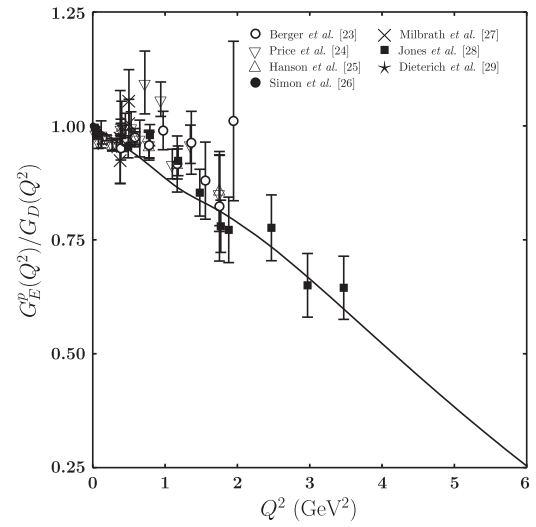


FIG. 16. Ratio $G_E^p(Q^2)/G_D(Q^2)$.

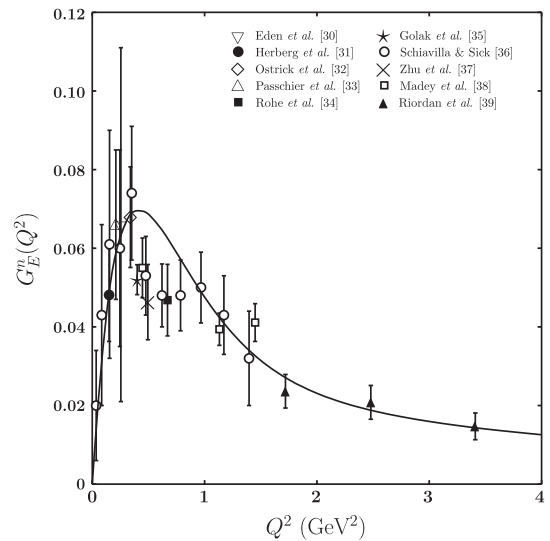
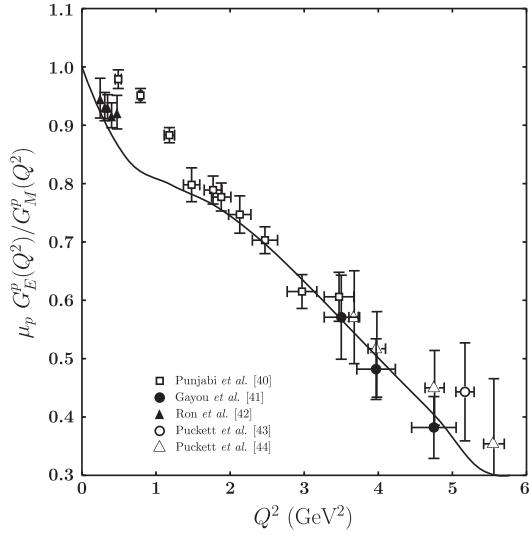


FIG. 17. Charge neutron form factor $G_E^n(Q^2)$.


 FIG. 18. Ratio $\mu_p G_E^p(Q^2)/G_M^p(Q^2)$.

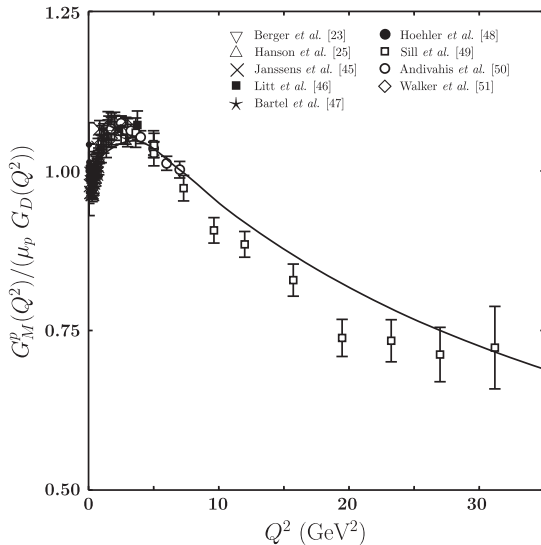
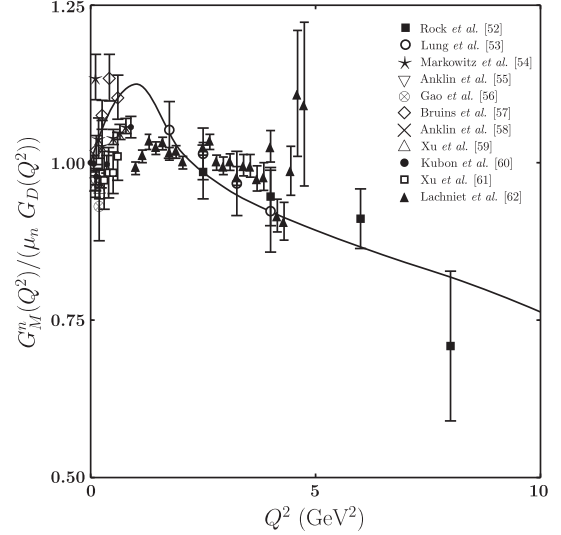
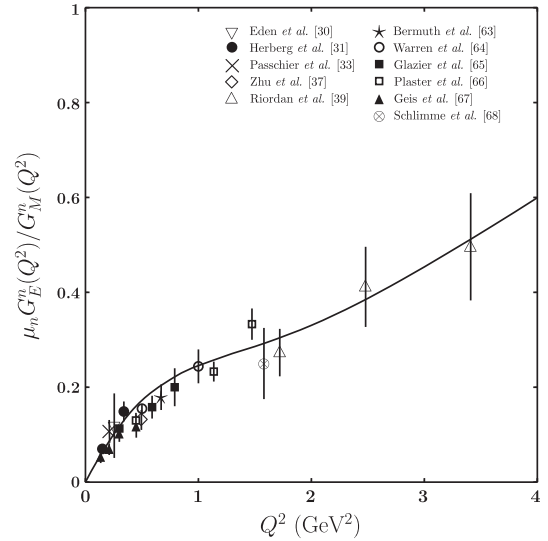
$$\Delta_q^{(1)} = \frac{1 + \eta_q^{(2)}}{2(1 + \bar{\eta}_q^{(2)})} - 1,$$

$$\Delta_q^{(2)} = \frac{2}{3}\Delta_q^{(1)} + \frac{1}{3}\left(\frac{1 + \sigma_q/2}{1 + \bar{\eta}_q^{(2)}} - 1\right) \quad (18)$$

and vanish for

$$\bar{\eta}_q^{(2)} = \frac{\sigma_q}{2} = \frac{\eta_q^{(2)} - 1}{2}. \quad (19)$$

The last limit is consistent with the Drell-Yan-West duality [21] relating the large- Q^2 behavior of nucleon electromagnetic form factors and the large- x behavior of the structure functions. However, a fine-tuned fit to the electromagnetic


 FIG. 19. Ratio $G_M^p(Q^2)/(\mu_p G_D(Q^2))$.

 FIG. 20. Ratio $G_M^n(Q^2)/(\mu_n G_D(Q^2))$.

 FIG. 21. Ratio $\mu_n G_E^n(Q^2)/G_M^n(Q^2)$.

form factors requires a deviation of $\Delta_q^{(i)}$ from zero with the numerical values of

$$\begin{aligned} \Delta_u^{(1)} &= 0.365, & \Delta_d^{(1)} &= 0.233, \\ \Delta_u^{(2)} &= 0.338, & \Delta_d^{(2)} &= 0.081. \end{aligned} \quad (20)$$

III. RESULTS

Finally, we discuss our numerical results for electromagnetic properties of nucleons. The fit results in values for the magnetic moments in terms of the nuclear magneton (n.m.) and for the electromagnetic radii as shown in Table II, we also show the current data [22] on these quantities. In Figs. 9–15 we present the plots of the Dirac

and Pauli form factors for u and d quarks and nucleons. The data in Figs. 9–15 are taken from Refs. [6,7]. In Figs. 16–21 we also give results for the Sachs nucleon form factors and compare them with the dipole formula $G_D(Q^2) = 1/(1 + Q^2/0.71 \text{ GeV}^2)^2$ and with data [23–68]. Overall we have good agreement with the data.

IV. CONCLUSION

In conclusion, we want to summarize the main result of our paper. Using global fits of valence u and d quark parton distributions and data on quark and nucleon form factors in the Euclidean region, we construct a light-front quark model for the nucleon structure consistent with model-independent scaling laws—the Drell-Yan-West duality [21] and quark counting rules [2].

ACKNOWLEDGMENTS

The authors thank Werner Vogelsang for the useful discussions. This work was supported by the DFG under Contract No. LY 114/2-1, by the German Bundesministerium für Bildung und Forschung (BMBF) under Grant No. 05P12VTCTG, by Marie Curie Reintegration Grant No. IRG 256574, by CONICYT (Chile) Research Project No. 80140097, by CONICYT (Chile) under Grant No. 7912010025, by FONDECYT (Chile) under Grants No. 1140390 and No. 1141280, and by the Tomsk State University Competitiveness Improvement Program. V.E.L. would like to thank the Departamento de Física y Centro Científico Tecnológico de Valparaíso (CCTVal), Universidad Técnica Federico Santa María, Valparaíso, Chile for the warm hospitality.

-
- [1] T. Gutsche, V.E. Lyubovitskij, I. Schmidt, and A. Vega, Light-front quark model consistent with Drell-Yan-West duality and quark counting rules, *Phys. Rev. D* **89**, 054033 (2014).
- [2] S.J. Brodsky and G.R. Farrar, Scaling Laws at Large Transverse Momentum, *Phys. Rev. Lett.* **31**, 1153 (1973); V.A. Matveev, R.M. Muradian, and A.N. Tavkhelidze, Automodellism in the large-angle elastic scattering and structure of hadrons, *Lett. Nuovo Cimento* **7**, 719 (1973).
- [3] A.D. Martin, W.J. Stirling, R.S. Thorne, and G. Watt, Parton distributions for the LHC, *Eur. Phys. J. C* **63**, 189 (2009).
- [4] M. Aicher, A. Schafer, and W. Vogelsang, Soft-Gluon Resummation and the Valence Parton Distribution Function of the Pion, *Phys. Rev. Lett.* **105**, 252003 (2010).
- [5] T. Gutsche, V.E. Lyubovitskij, I. Schmidt, and A. Vega, Pion light-front wave function, parton distribution and the electromagnetic form factor, [arXiv:1410.6424](https://arxiv.org/abs/1410.6424).
- [6] G.D. Cates, C.W. de Jager, S. Riordan, and B. Wojtsekhowski, Flavor Decomposition of the Elastic Nucleon Electromagnetic Form Factors, *Phys. Rev. Lett.* **106**, 252003 (2011).
- [7] M. Diehl and P. Kroll, Nucleon form factors, generalized parton distributions and quark angular momentum, *Eur. Phys. J. C* **73**, 2397 (2013); M. Diehl, Generalized parton distributions from form factors, *Nucl. Phys. B, Proc. Suppl.* **161**, 49 (2006).
- [8] I.T. Obukhovskiy, A. Faessler, T. Gutsche, and V.E. Lyubovitskij, Electromagnetic structure of the nucleon and the Roper resonance in a light-front quark approach, *Phys. Rev. D* **89**, 014032 (2014); Light quark contributions to the nucleon electromagnetic form factors, *J. Phys. G* **41**, 095005 (2014).
- [9] M. Diehl, T. Feldmann, R. Jakob, and P. Kroll, Generalized parton distributions from nucleon form-factor data, *Eur. Phys. J. C* **39**, 1 (2005); M. Guidal, M.V. Polyakov, A.V. Radyushkin, and M. Vanderhaeghen, Nucleon form factors from generalized parton distributions, *Phys. Rev. D* **72**, 054013 (2005); O.V. Selyugin and O.V. Teryaev, Generalized parton distributions and description of electromagnetic and graviton form factors of nucleon, *Phys. Rev. D* **79**, 033003 (2009).
- [10] A.V. Radyushkin, Nonforward parton densities and soft mechanism for form-factors and wide angle Compton scattering in QCD, *Phys. Rev. D* **58**, 114008 (1998).
- [11] D. Mueller, D. Robaschik, B. Geyer, F.M. Dittes, and J. Horejsi, Wave functions, evolution equations and evolution kernels from light-ray operators of QCD, *Fortschr. Phys.* **42**, 101 (1994); X.D. Ji, Gauge Invariant Decomposition of Nucleon Spin, *Phys. Rev. Lett.* **78**, 610 (1997); A.V. Radyushkin, Nonforward parton distributions, *Phys. Rev. D* **56**, 5524 (1997).
- [12] S.J. Brodsky and S.D. Drell, The anomalous magnetic moment and limits on fermion substructure, *Phys. Rev. D* **22**, 2236 (1980).
- [13] S.J. Brodsky and D.S. Hwang, Exact light cone wave function representation of matrix elements of electroweak currents, *Nucl. Phys.* **B543**, 239 (1999); S.J. Brodsky, D.S. Hwang, B.-Q. Ma, and I. Schmidt, Light cone representation of the spin and orbital angular momentum of relativistic composite systems, *Nucl. Phys.* **B593**, 311 (2001); S.J. Brodsky, M. Diehl, and D.S. Hwang, Light cone wave function representation of deeply virtual Compton scattering, *Nucl. Phys.* **B596**, 99 (2001).
- [14] S.J. Brodsky and G.F. de Teramond, Light-front dynamics and AdS/QCD correspondence: The pion form factor in the space- and time-like regions, *Phys. Rev. D* **77**, 056007 (2008); G.F. de Teramond and S.J. Brodsky, Excited baryons in holographic QCD, *AIP Conf. Proc.* **1432**, 168 (2012); S.J. Brodsky and G.F. de Teramond, Applications of AdS/QCD and light-front holography to baryon physics, *AIP Conf. Proc.* **1388**, 22 (2011).
- [15] S.J. Brodsky, F.-G. Cao, and G.F. de Teramond, Meson transition form factors in light-front holographic QCD, *Phys. Rev. D* **84**, 075012 (2011).

- [16] Z. Abidin and C. E. Carlson, Nucleon electromagnetic and gravitational form factors from holography, *Phys. Rev. D* **79**, 115003 (2009).
- [17] A. Vega, I. Schmidt, T. Branz, T. Gutsche, and V. E. Lyubovitskij, Meson wave function from holographic models, *Phys. Rev. D* **80**, 055014 (2009); T. Branz, T. Gutsche, V. E. Lyubovitskij, I. Schmidt, and A. Vega, Light and heavy mesons in a soft-wall holographic approach, *Phys. Rev. D* **82**, 074022 (2010); T. Gutsche, V. E. Lyubovitskij, I. Schmidt, and A. Vega, Chiral symmetry breaking and meson wave functions in soft-wall AdS/QCD, *Phys. Rev. D* **87**, 056001 (2013).
- [18] T. Gutsche, V. E. Lyubovitskij, I. Schmidt, and A. Vega, Dilaton in a soft-wall holographic approach to mesons and baryons, *Phys. Rev. D* **85**, 076003 (2012); Nucleon structure including high Fock states in AdS/QCD, *Phys. Rev. D* **86**, 036007 (2012); Nucleon resonances in AdS/QCD, *Phys. Rev. D* **87**, 016017 (2013).
- [19] S. J. Brodsky, M. Burkardt, and I. Schmidt, Perturbative QCD constraints on the shape of polarized quark and gluon distributions, *Nucl. Phys.* **B441**, 197 (1995).
- [20] F. Yuan, Generalized parton distributions at $x \rightarrow 1$, *Phys. Rev. D* **69**, 051501 (2004).
- [21] S. D. Drell and T.-M. Yan, Connection of Elastic Electromagnetic Nucleon Form-Factors at Large Q^2 and Deep Inelastic Structure Functions Near Threshold, *Phys. Rev. Lett.* **24**, 181 (1970); G. B. West, Phenomenological Model for the Electromagnetic Structure of the Proton, *Phys. Rev. Lett.* **24**, 1206 (1970).
- [22] K. A. Olive *et al.* (Particle Data Group Collaboration), Review of particle physics, *Chin. Phys. C* **38**, 090001 (2014).
- [23] C. Berger, V. Burkert, G. Knop, B. Langenbeck, and K. Rith, Electromagnetic form-factors of the proton at squared four momentum transfers between 10 fm^{-2} and 50 fm^{-2} , *Phys. Lett.* **35B**, 87 (1971).
- [24] L. E. Price, J. Dunning, M. Goitein, K. Hanson, T. Kirk, and R. Wilson, Backward-angle electron-proton elastic scattering and proton electromagnetic form factors, *Phys. Rev. D* **4**, 45 (1971).
- [25] K. M. Hanson, J. Dunning, M. Goitein, T. Kirk, L. Price, and R. Wilson, Large angle quasielastic electron-deuteron scattering, *Phys. Rev. D* **8**, 753 (1973).
- [26] G. G. Simon, C. Schmitt, F. Borkowski, and V. H. Walther, Absolute electron proton cross-sections at low momentum transfer measured with a high pressure gas target system, *Nucl. Phys.* **A333**, 381 (1980).
- [27] B. D. Milbrath *et al.* (Bates FPP Collaboration), Comparison of Polarization Observables in Electron Scattering from the Proton and Deuteron, *Phys. Rev. Lett.* **80**, 452 (1998); **82**, 2221(E) (1999).
- [28] M. K. Jones *et al.* (Jefferson Lab Hall A Collaboration), G_{E_p}/G_{M_p} Ratio by Polarization Transfer in $\vec{e}p \rightarrow e\vec{p}$, *Phys. Rev. Lett.* **84**, 1398 (2000).
- [29] S. Dieterich *et al.*, Polarization transfer in the $^4\text{He}(\vec{e}, e'\vec{p})^3\text{H}$ reaction, *Phys. Lett. B* **500**, 47 (2001).
- [30] T. Eden *et al.*, Electric form factor of the neutron from the $^2\text{H}(\vec{e}e'\vec{n})^1\text{H}$ reaction at $Q^2 = 0.255 (\text{GeV}/c)^2$, *Phys. Rev. C* **50**, R1749 (1994).
- [31] C. Herberg *et al.*, Determination of the neutron electric form-factor in the $D(e, e'n)p$ reaction and the influence of nuclear binding, *Eur. Phys. J. A* **5**, 131 (1999).
- [32] M. Ostrick *et al.*, Measurement of the Neutron Electric Form Factor G_{E_n} in the Quasifree $^2\text{H}(\vec{e}, e'\vec{n})p$ Reaction, *Phys. Rev. Lett.* **83**, 276 (1999).
- [33] I. Passchier *et al.*, Charge Form Factor of the Neutron from the Reaction $^2\text{H}(\vec{e}, e'n)p$, *Phys. Rev. Lett.* **82**, 4988 (1999).
- [34] D. Rohe *et al.*, Measurement of the Neutron Electric Form Factor G_{en} at $0.67 (\text{GeV}/c)^2$ via $^3\text{He}(\vec{e}, e'n)$, *Phys. Rev. Lett.* **83**, 4257 (1999).
- [35] J. Golak, G. Ziemer, H. Kamada, H. Witala, and W. Glöckle, Extraction of electromagnetic neutron form factors through inclusive and exclusive polarized electron scattering on polarized ^3He target, *Phys. Rev. C* **63**, 034006 (2001).
- [36] R. Schiavilla and I. Sick, Neutron charge form factor at large q^2 , *Phys. Rev. C* **64**, 041002 (2001).
- [37] H. Zhu *et al.* (Jefferson Lab E93-026 Collaboration), Measurement of the Electric Form Factor of the Neutron through $\vec{d}(\vec{e}, e'n)p$ at $Q^2 = 0.5 (\text{GeV}/c)^2$, *Phys. Rev. Lett.* **87**, 081801 (2001).
- [38] R. Madey *et al.* (Jefferson Lab E93-038 Collaboration), Measurements of G_E^n/G_M^n from the $^2\text{H}(\vec{e}, e'\vec{n})^1\text{H}$ Reaction to $Q^2 = 1.45 (\text{GeV}/c)^2$, *Phys. Rev. Lett.* **91**, 122002 (2003).
- [39] S. Riordan *et al.*, Measurements of the Electric Form Factor of the Neutron up to $Q^2 = 3.4 \text{ GeV}^2$ Using the Reaction $^3\text{He}(\vec{e}, e'n)pp$, *Phys. Rev. Lett.* **105**, 262302 (2010).
- [40] V. Punjabi *et al.*, Proton elastic form factor ratios to $Q^2 = 3.5 \text{ GeV}^2$ by polarization transfer, *Phys. Rev. C* **71**, 055202 (2005); **71**, 069902(E) (2005).
- [41] O. Gayou *et al.* (Jefferson Lab Hall A Collaboration), Measurement of G_{E_p}/G_{M_p} in $\vec{e}p \rightarrow e\vec{p}$ to $Q^2 = 5.6 \text{ GeV}^2$, *Phys. Rev. Lett.* **88**, 092301 (2002).
- [42] G. Ron *et al.* (Jefferson Lab Hall A Collaboration), Low Q^2 measurements of the proton form factor ratio $\mu_p G_E/G_M$, *Phys. Rev. C* **84**, 055204 (2011).
- [43] A. J. R. Puckett *et al.*, Recoil Polarization Measurements of the Proton Electromagnetic Form Factor Ratio to $Q^2 = 8.5 \text{ GeV}^2$, *Phys. Rev. Lett.* **104**, 242301 (2010).
- [44] A. J. R. Puckett *et al.*, Final analysis of proton form factor ratio data at $Q^2 = 4.0, 4.8$ and 5.6 GeV^2 , *Phys. Rev. C* **85**, 045203 (2012).
- [45] T. Janssens, R. Hofstadter, E. B. Hughes, and M. R. Yearian, Proton form factors from elastic electron-proton scattering, *Phys. Rev.* **142**, 922 (1966).
- [46] J. Litt *et al.*, Measurement of the ratio of the proton form factors, G_E/G_M , at high momentum transfers and the question of scaling, *Phys. Lett.* **31B**, 40 (1970).
- [47] W. Bartel, F.-W. Büsser, W.-R. Dix, R. Felst, D. Harms, H. Krehbiel, P. E. Kuhlmann, J. McElroy, J. Meyer, and G. Weber, Measurement of proton and neutron electromagnetic form-factors at squared four momentum transfers up to $3 (\text{GeV}/c)^2$, *Nucl. Phys.* **B58**, 429 (1973).
- [48] G. Hohler, E. Pietarinen, I. Sabba-Stefanescu, F. Borkowski, G. G. Simon, V. H. Walther, and R. D. Wendling, Analysis of electromagnetic nucleon form-factors, *Nucl. Phys.* **B114**, 505 (1976).

- [49] A. F. Sill *et al.*, Measurements of elastic electron-proton scattering at large momentum transfer, *Phys. Rev. D* **48**, 29 (1993).
- [50] L. Andivahis *et al.*, Measurements of the electric and magnetic form factors of the proton from $Q^2 = 1.75$ (GeV/c)² to 8.83 (GeV/c)², *Phys. Rev. D* **50**, 5491 (1994).
- [51] R. C. Walker *et al.*, Measurements of the proton elastic form factors for $1 \leq Q^2 \leq 3$ (GeV/c)² at SLAC, *Phys. Rev. D* **49**, 5671 (1994).
- [52] S. Rock, R. Arnold, P. Bosted, B. Chertok, B. Mecking, I. Schmidt, Z. Szalata, R. York, and R. Zdarko, Measurement of Elastic Electron-Neutron Cross Sections up to $Q^2 = 10$ (GeV/c)², *Phys. Rev. Lett.* **49**, 1139 (1982).
- [53] A. Lung *et al.*, Measurements of the Electric and Magnetic Form Factors of the Neutron from $Q^2 = 1.75$ (GeV/c)² to 4 (GeV/c)², *Phys. Rev. Lett.* **70**, 718 (1993).
- [54] P. Markowitz *et al.*, Measurement of the magnetic form factor of the neutron, *Phys. Rev. C* **48**, R5 (1993).
- [55] H. Anklin *et al.*, Precision measurement of the neutron magnetic form factor, *Phys. Lett. B* **336**, 313 (1994).
- [56] H. Gao *et al.*, Measurement of the neutron magnetic form factor from inclusive quasielastic scattering of polarized electrons from polarized ³He, *Phys. Rev. C* **50**, R546 (1994).
- [57] E. E. W. Bruins *et al.*, Measurement of the Neutron Magnetic Form Factor, *Phys. Rev. Lett.* **75**, 21 (1995).
- [58] H. Anklin *et al.*, Precise measurements of the neutron magnetic form factor, *Phys. Lett. B* **428**, 248 (1998).
- [59] W. Xu *et al.*, Transverse Asymmetry A_T from the Quasielastic ³He(\vec{e}, e') Process and the Neutron Magnetic Form Factor, *Phys. Rev. Lett.* **85**, 2900 (2000).
- [60] G. Kubon *et al.*, Precise neutron magnetic form factors, *Phys. Lett. B* **524**, 26 (2002).
- [61] W. Xu *et al.* (Jefferson Lab E95-001 Collaboration), PWIA extraction of the neutron magnetic form factor from quasielastic ³He(\vec{e}, e') at $Q^2 = 0.3$ (GeV/c)² to 0.6 (GeV/c)², *Phys. Rev. C* **67**, 012201 (2003).
- [62] V. J. Lachniet *et al.* (CLAS Collaboration), A Precise Measurement of the Neutron Magnetic Form Factor G_M^n in the Few-GeV² Region, *Phys. Rev. Lett.* **102**, 192001 (2009).
- [63] J. Bermuth *et al.*, The neutron charge form-factor and target analyzing powers from ³He($\vec{e}, e'n$) scattering, *Phys. Lett. B* **564**, 199 (2003).
- [64] G. Warren *et al.* (Jefferson Laboratory E93-026 Collaboration), Measurement of the Electric Form Factor of the Neutron at $Q^2 = 0.5$ and 1.0 GeV²/c², *Phys. Rev. Lett.* **92**, 042301 (2004).
- [65] D. I. Glazier *et al.*, Measurement of the electric form-factor of the neutron at $Q^2 = 0.3$ (GeV/c)² to 0.8 (GeV/c)², *Eur. Phys. J. A* **24**, 101 (2005).
- [66] B. Plaster *et al.* (Jefferson Laboratory E93-038 Collaboration), Measurements of the neutron electric to magnetic form factor ratio G_{E_n}/G_{M_n} via the ²H($\vec{e}, e'n$)¹H reaction to $Q^2 = 1.45$ (GeV/c)², *Phys. Rev. C* **73**, 025205 (2006).
- [67] E. Geis *et al.* (BLAST Collaboration), Charge Form Factor of the Neutron at Low Momentum Transfer from the ²H($\vec{e}, e'n$)¹H Reaction, *Phys. Rev. Lett.* **101**, 042501 (2008).
- [68] B. S. Schlimme *et al.*, Measurement of the Neutron Electric to Magnetic Form Factor Ratio at $Q^2 = 1.58$ GeV² Using the Reaction ³He($\vec{e}, e'n$) pp , *Phys. Rev. Lett.* **111**, 132504 (2013).